NIOBIUM MICROALLOYED CA-50 REBARS – DEVELOPMENT AND CHARACTERIZATION*

Ana Clara Fonseca da Silva[1]
Tiago Seixas Bittencourt[2]
Beatriz Pereda[3]
Beatriz Lopez[3]
Marcelo Arantes Rebellato[4]
Andre Luiz Vasconcellos da Costa e Silva[5]

Abstract
Reinforcing steel bars are usually specified based on mechanical properties with flexibility in chemical composition and processing. Most developments, in these steels, are normally focused on alloy and process design to reach minimum cost and conformity to specification. Processing routes using quenching and self-tempering (QST) and accelerated cooling are the most common. Microalloying with V and Nb have been used in rebar. When acicular constituents must be avoided, a combination of Nb microalloying with judicious control of cooling is one of the preferred options. Niobium can contribute to improvement in tensile properties through austenitic grain size control during hot working, precipitation hardening due to carbonitrides or clusters, and hardenability increase. In the present work the alloy design and development processes of a Nb microalloyed steel for rebars are presented. The designed steel has fulfilled the required specification and is under regular production. Austenitic grain size refining – when comparing with the "basic composition" normally used was observed, even without any change in the thermomechanical processing cycle. There are indications that precipitation hardening may also occur. Results indicate that Nb is a good alternative as a microalloying element in rebars.
Keywords: Niobium; Rebar; Vanadium; Precipitation.

1 *Metallurgical Engineer, EEIMVR-UFF, Volta Redonda, Brazil.*
2 *Metallurgical Engineer, MSc, CSN, Volta Redonda, Brazil.*
3 *Dr, CEIT, San Sebastian, Spain*
4 *Metallurgical Engineer, CBMM, São Paulo, Brazil*
5 *Metallurgical Engineer, PhD Professor, EEIMVR-UFF, Volta Redonda, Brazil*

1 INTRODUCTION

Reinforcing steel bars are normally specified based on mechanical properties (e.g.(1)). Most standards are flexible with respect to chemical composition and processing. Only when weldability is to be guaranteed, some chemical composition limitations are imposed (e.g (2)). Most developments, in these steels, focus on alloy and process design to reach minimum cost and conformity to specification (3) (4) (5). Processing routes using quenching and self-tempering (QST) (6) and accelerated cooling (7) are the most common. Microalloying with V and Nb have been used in rebar (4) (5) (8) (9) (10). When acicular constituents must be avoided, a combination of Nb microalloying with judicious control of cooling is one of the preferred options. Niobium can contribute to improvement in tensile properties through austenitic grain size control during hot working, precipitation hardening due to carbonitrides or clusters, and hardenability increase (5) (11) (12).
In the present work the alloy design and development processes of an Nb microalloyed steel for rebars are presented. The steel is characterized and compared with the previously used V microalloyed steel. For the processing characterization, we compared the hot rolling behavior via hot torsion (13) (14): two different cooling schedules were simulated, too. Dilatometric tests and microstructural characterization in different scales was also performed. The objective of the tests was to further understand (3) the behavior of the new steel and compare it with the steel that was previously used.

2 MATERIAL AND METHODS

2.1 Steels

Industrial heats of two rebar steels were used for the tests. Their chemical compositions are present in the Figure 1. The steels were continuously cast in square billets.

Sample	%C	%Mn	%Si	%V/Nb
V steel	0.34	1.18	0.214	0.030
Nb steel	0.35	1.15	0.183	0.025

Figure 1. Steels chemical composition

The content of residual elements was approximately the same for both steels.
The work was conducted in laboratory scale. First of all torsion tests were performed using industrial schedule parameters with two different cooling rate: cycle 1 – air cooling and cycle 2 – accelerated cooling (Steelmor) simulation.
The samples microstructure was characterized using 2% Nital. In order to investigate the precipitation, the microstructure was analyzed after reheating (the reheating temperature considered was 1100ºC), after hot deformation and after austenite decomposition. Hardness values was measured in both steels in order to evaluate the influence of the cooling rate.
TEM analyzes was performed in the Nb steel in order to investigate the precipitation during and after the hot deformation. For this analyzes the samples was obtained after reheating, after hot deformation and after the austenite decomposition. The Figure 2 shows the cycle adopted for the selection of the samples.

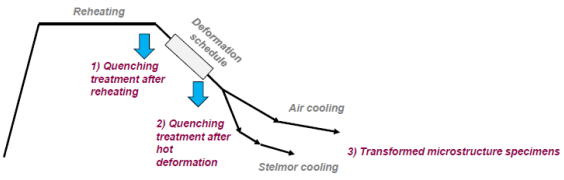

Figure 2. Cycle adopted to selected TEM analyzes samples.

2.2 Torsion Test

The torsion tests were programed to replicate the hot rolling deformation-temperature schedule. The reheating temperature considered was 1160ºC.

2.3 Metalography

Metallographic specimens were observed in conventional optical microscopy. Selected samples were thinned and extracted in a SEM-FIB for TEM observation. Most of the carbonitride observation was made incarbon extraction replicas observed in TEM.

3 RESULTS AND DISCUSSION

3.1 Hot Torsion tests

The deformation schedule in the hot torsion test was based on the industrial rolling schedule. For both steels, samples at the end of the deformation cycle (approx. 962ºC) were quenched in order to evaluate the austenite microstruture before phase transformation.

The stress-strain curves under torsion are shown in the Figure 3. The shape of the curves is similar for both steels. For both steels, one can observe that the beginning of dynamic recrystallization occurs after pass 17, when the interval between passes decreases to 0.5s.

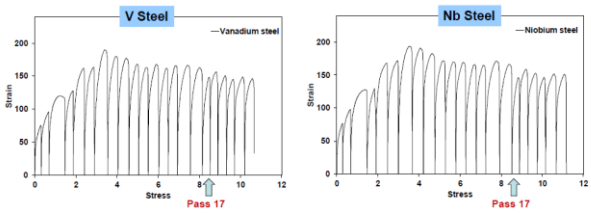

Figure 3. Stress-strain curves for V and Nb steel.

The mean flow stress during deformation is also similar for both steels. The Nb steel presented values somewhat higher, as indicated in Figure 4.

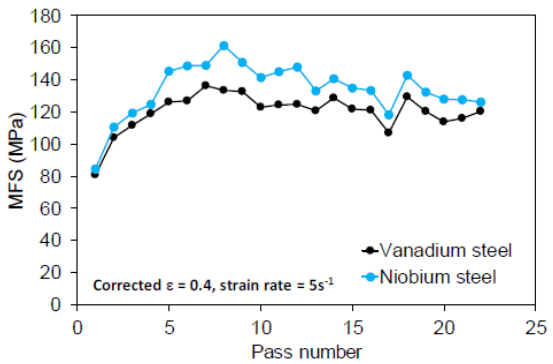

Figure 4. Mean flow stress for Nb and V steel.

3.2 Austenitic microstructure after reheating

After reheating to around 1100ºC, Nb steel samples were quenched to study the austenite microstructure after reheating. Figure 5 presents the micrographs: large grains and a significant heterogeneity of austenite grain size can be observed. This indicates abnormal grain growth, probably associated to partial dissolution of precipitates that could control the austenitic grain size. This is confirmed by thermodynamic calculations (3)

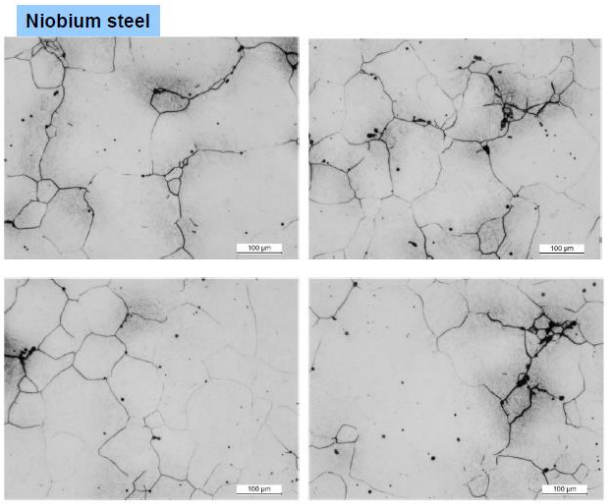

Figure 5. Optical micrograph of samples of the Nb steel heated to the soaking temperature and quenched. Etchant: Bechet-Beaujard. The austenitic grain is large and there is significant size heterogeneity.

3.2.2 Austenite microstructure after hot deformation

Nb and V steel samples were quenched after the hot deformation (from approximately 962ºC). Both steels presented equiaxial, fine austenite grains at this stage, as shown in Figure 6. Similar austenitic grain size distribution was observed in both steels. This is consistent with the suggestion of dynamic/metadynamic recrystallization during the final deformation stages, as shown in Figure 3.

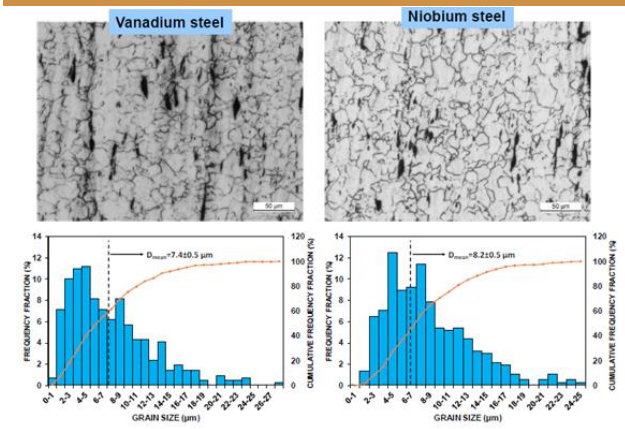

Figure 6. Optical micrograph of samples of Nb and V stees quenched after hot torsion test. Etchant: Bechet-Beaujard. Both steels present fine, equiaxial austenite grains.

3.3 Microstruture after austenite decomposition

The Nb steel samples subjected to air cooling or air accelerated cooling were etched with Nital 2% in order to show the phases presents and the ferrite grain size. Ferrite/perlite phases was observed in the Nb steel air cooled. However, a small fraction of acicular ferrite was also observed. Accelerated air cooling (Cycle 2, Stelmor) increased the acicular phase fraction and decreased the fraction of allotriomorphic ferrite. Figures 7 and 8 show the representative micrographs.

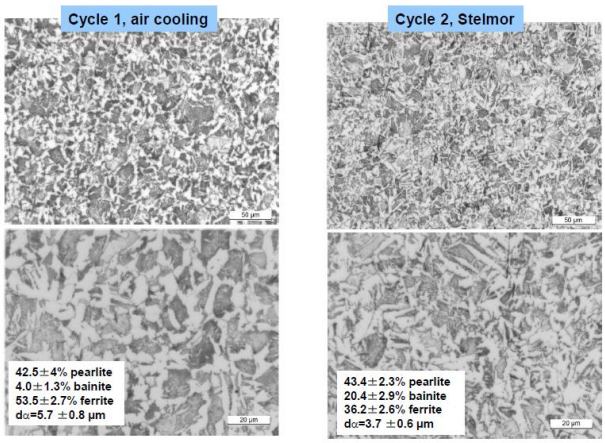

Figure 7. Nb steel samples subjected to air cooling and to accelerated air cooling (stelmor simulation). Nital 2%.

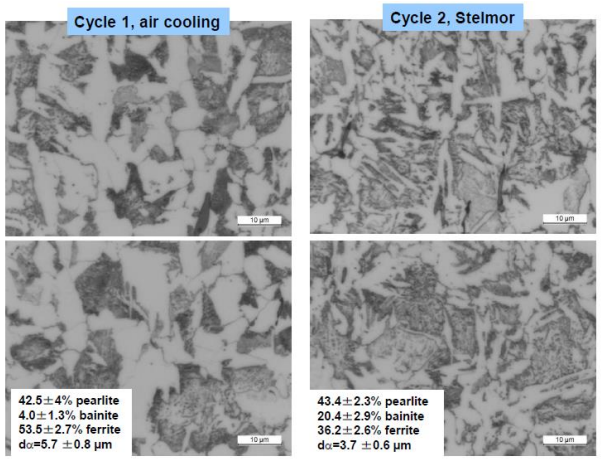

Figure 8. Nb steel samples quenched after the phase transformation. Nital 2%.

In the case of the V steel the air cooled sample presented a ferrite-perlite microstructure. Accelerated air cooling (cycle 2) introduced acicular constituents. (Figure 9 and 10).

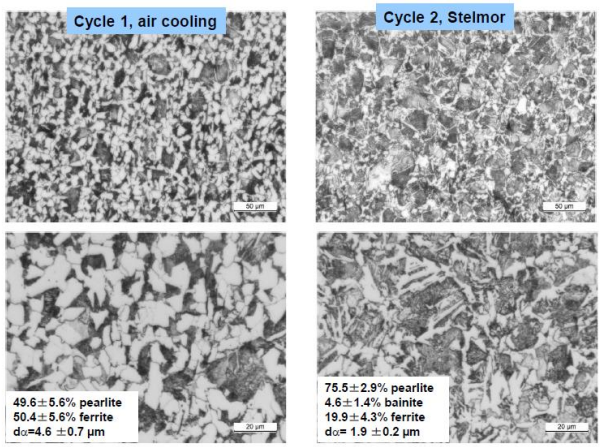

Figure 9. V steel sample quenched after phase transformation. Air cooling (cycle 1) accelerated air cooling(cycle 2). Nital 2%.

3.4 Comparison of V and Nb steel microstructures. Cycle 1: air cooling.

The comparation between the steels showed that the Nb steel microstructure was more acicular than that of the V steel, as shown in Figure 10.

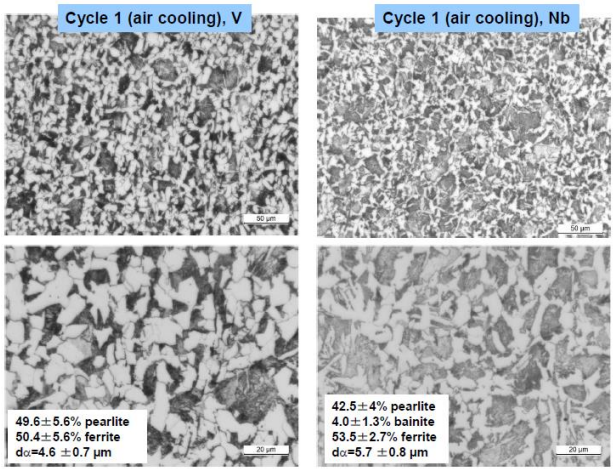

Figure 10. V e Nb steel air cooled. Cycle 1.

3.5 Comparison of V and Nb steel. Accelerated air cooling Cycle 2: Steelmor.

The steel microstructures obtained with the cycle 2 are similar. The volume fraction of acicular constituents is higher in the Nb steel (Figure 11).

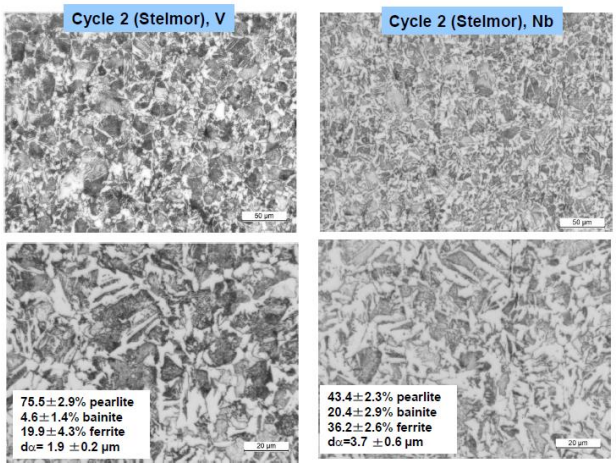

Figure 11. V and Nb steel accelerated air cooling. Cycle 2.

4 HARDNESS

HV1 hardness was measured along a line on a flat longitudinal plane at 0.9R from the center of the torsion specimen.

The Nb steel had homogeneous hardness in both cooling conditions. The values of hardness were not significantly affected by the accelerated cooling (Figure 12).

Sample	Mean	Min	Max	StdD	Range
Air cooling	222	207	236	10	29
Stelmor	221	209	231	8	22

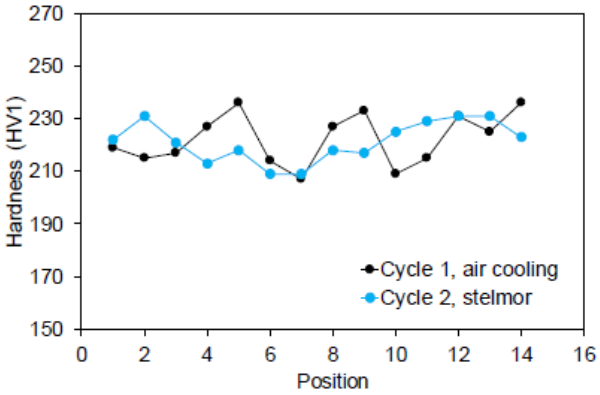

Figure 22. Nb steel hardness values

The V steel also presented uniform hardness, but the effect of accelerated cooling could be observed. (Figure 13).

Hardness, HV1:

Sample	Mean	Min	Max	StdD	Range
Air cooling	220	204	231	7.2	27
Stelmor	234	220	247	7.3	27

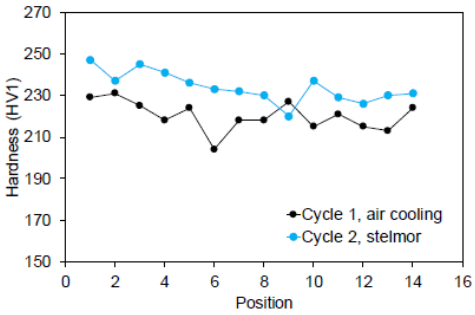

Figure 33. V hardness values.

Comparison of the hardness results between the steels seem to indicate a higher hardenability of the V steel when compared to the Nb steel.

5 TEM and SEM-FIB ANALYSIS

Only the Nb steel was examined by TEM to evaluate precipitates.

There sample conditions were examined:

1) After reheating – Samples were quenched after reheating and before

any hot working to analyze undissolved precipitates;

2) After hot deformation – samples were quenched right after the end of hot working to evaluate deformation induced precipitation.

3) After phase transformation (air cooling cycle only) – these samples were examined both by TEM (replicas) and in SEM-FIB to evaluate the precipitation during/after the phase transformation;

5.2 Samples quenched after reheating – Nb steel

Only relatively large precipitates and precipitate clusters where observed in this condition, in the Nb steel. Precipitate free areas were observed. Some of the larger clusters (not shown here) are caused by solidification segregation (3) (15). The smallest precipitate size observed was ≈ 20 nm. (Figure 14) This results together with the austenitic grain size heterogeneity (Figure 5) indicate a partial dissolution of the Nb during the reheating at 1160ºC as calculated by computational thermodynamics (3).

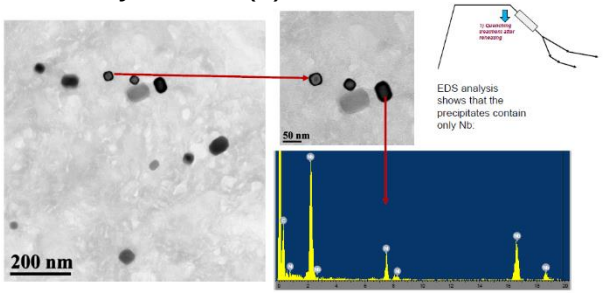

Figure 14. Precipitates in Nb steel reheated for hot working and quenched. (TEM, carbon replicas)

5.3 Samples quenched after hot deformation

Precipitate free areas were also observed in this condition. The undissolved precipitates were once more observed, as expected.

In some areas it was possible to observe fine precipitates. These particles probably formed during hot deformation, by deformation induced precipitation (16) (17).

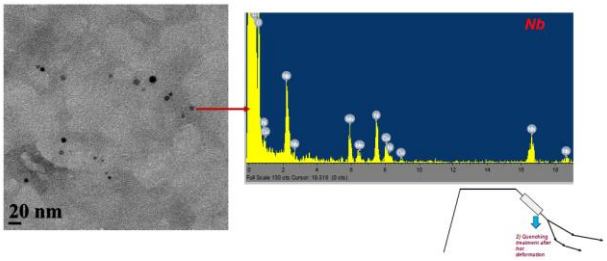

Figure 15. Fine precipitates in Nb steel quenched after hot deformation (carbon replica).

The results showed some limited precipitation induced by deformation. The deformation induced precipitation was not sufficient to inhibit recrystallization in the last passes of hot working and the final austenitic grains are equiaxed (Figure 16).

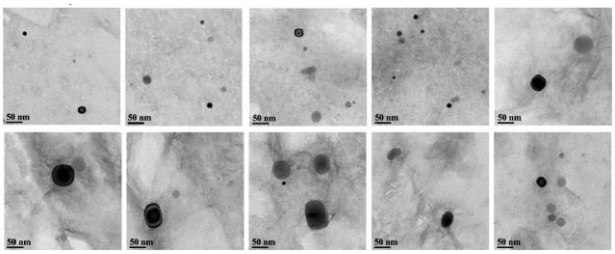

Figure 16. Equiaxial austenite grain. Carbon replicas samples quenched after hot deformation.

5.4 Samples quenched after air cooling

The amount of precipitates in this sample was larger than in the previous ones. In addition, a large amount of fine precipitates was observed. This suggest additional precipitation during the cooling. These precipitates are shown in Figure 17.

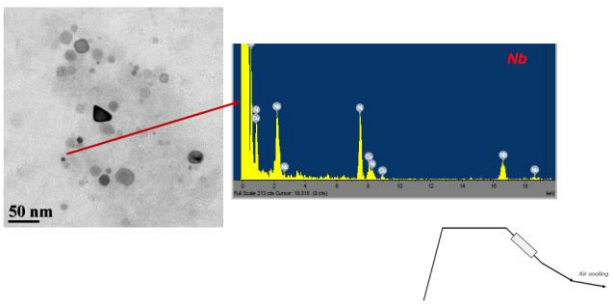

Figure 17. Fine precipitates in air cooled Nb steel (carbon replica)

Some of the carbonitrides are very fine and could contribute to precipitation hardening (<10nm). These precipitated formed either during or after phase transformation (18) (19).

5.5 Samples quenched after simulation of Stelmor cooling

The precipitation in the sample quenched after Stelmor cooling simulation (cycle 2) was like that observed in the air cooled sample.
As the air cooled sample, the amount of precipitates is not abundant and some are not in the ideal size to influence properties. (Figure 18).

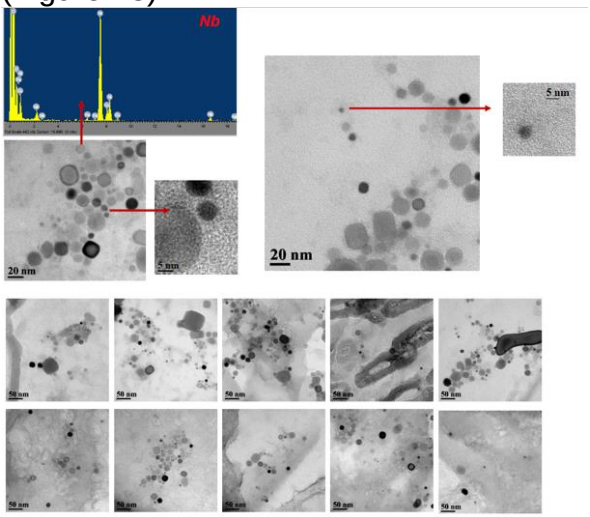

Figure 18. Fine precipitates in Nb steel with Stelmor cooling simulation.

5.5.1 Air cooled samples- microstructure analysis

Samples were removed using SEM-FIB and thinned for TEM examination from pearlite and ferrite -pearlite regions (Figure 19).

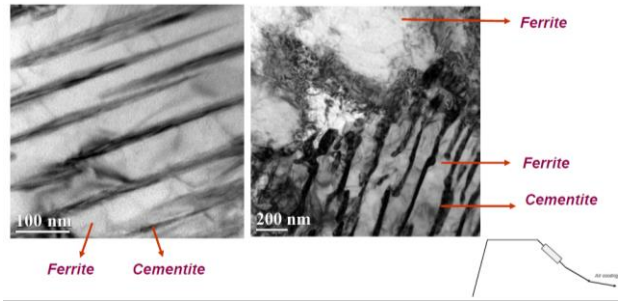

Figure 4. Microstructure of Nb steel air cooled. TEM bright field.

In the ferrite areas, a significant amount of dislocations can be observed. Dispersed precipitates in the same range size found in the carbon replicas can be seen in these samples (Figure 20).

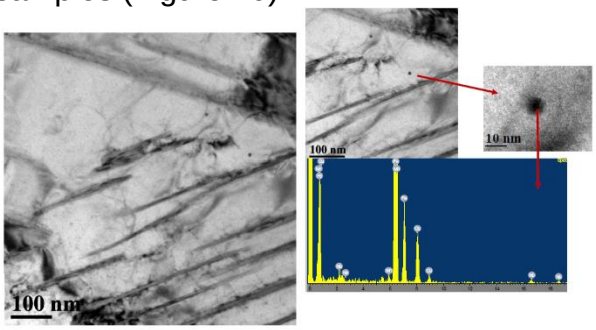

Figure 5. TEM of Nb steel air cooled. Dislocations and precipitates.

Dark field imagining was used in order to try detecting more precipitates with the same orientation in the same area (Figure 21).

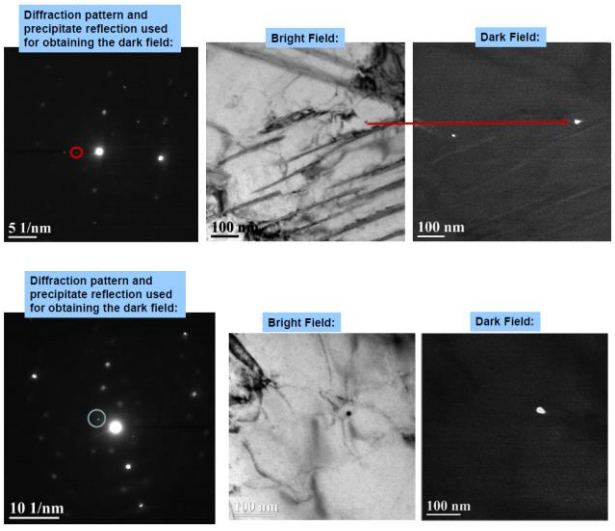

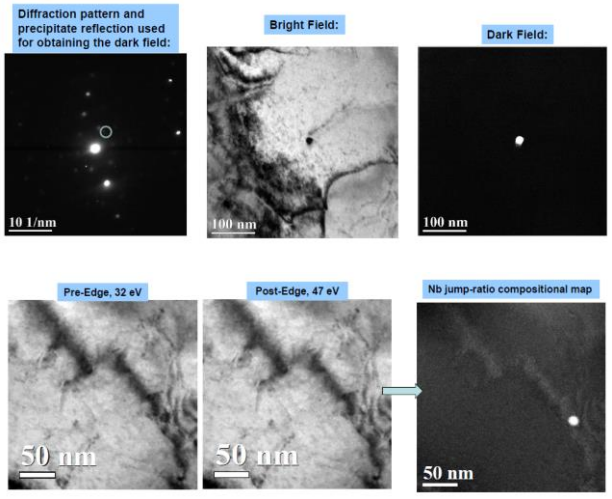

Figure 6. Nb steel air cooled. TEM Dark field image.

The actual distribution of the carbonitrides can be better estimated from these thin foils than from the replicas.

6 CONCLUSIONS

The deformation behavior of the Nb steel and V steel in the hot torsion tests were similar. Hot torsion indicates the onset of dynamic recrystallization on the last rolling passes.

Both steels had, after hot deformation, similar austenite structure: equiaxial with similar size (≈ 8 μm).

Air cooling the V steel lead to a ferrite-pearlite microstructure. On the other hand, the Nb steel presented some acicular constituents. (a volume fraction of around 4%).

Similar hardness values were obtained with the Nb steel air cooled and under Stelmor simulation (220HV).

The simulated Stelmor cooling led to the formation of a volume fraction of around 20% of acicular constituent in the V steel, with a corresponding hardness increase to around 235HV.

TEM analysis of the Nb steel has shown that there is partial dissolution of the carbonitrides when heating for hot working. During hot working there was some deformation induced precipitation, but this was insufficient to stop recrystallization. Significant austenitic grain growth occurred during heating for hot torsion in both steels. In the carbon replicas obtained by the air cooling and Stelmor cooling Nb samples, the amount of thin precipitates increases, showed that some precipitation occurs during the final cooling or during/after the phase transformation. However, it was not possible to detect difference between the precipitates found in both samples.

Somewhat more extensive precipitation of fine carbonitrides was found in the air cooled and Stelmor simulation sample of the Nb-steel. This indicates that there is probably some contribution to strength from dispersion hardening.

Acknowledgments

The authors thank CSN and CBMM for making this work possible.

REFERENCES

1. ABNT. ABNT NBR 7480:2007 Aço destinado a armaduras para estruturas de concreto armado - Especificação. São Paulo; 2007.

2. ABNT. ABNT NBR 8965:1985 Barras de aço CA 42 S com características de soldabilidade destinadas a armaduras para concreto armado - Especificação. São Paulo; 1985.

3. A Costa e Silva, ACF Silva, TS Bittencourt. Caracterização preliminar de um aço microligado ao Nb para vergalhão de construção civil In: ABM Week 2018 Proceedings [Internet]. São Paulo: Editora Blucher; 2018. p. 496–506.

4. W Chen, J Cao, Y Yang, Z Shi, W Zhang, M Huang. Investigation on the Strengthening and Toughening Mechanism of 500 MPa V-Nb Microalloyed Anti-Seismic Rebars. Materials Science. 2015;21(4):536–42.

5. Y Zhang, A Guo, Q Yong. Strengthening Effects of Niobium on High Strength Rebars. Journal of Mechanics Engineering and Automation 2018;8(2) 82-91

6. M Economopoulos, Y Respen, G Lessel, G Steffes. Application of the Tempcore Process to the Fabrication of High Yield Strenght Concrete-reinforcing Bars. CRM Revue. 1975;(45):1–17.

7. H Colpaert. Metallography of steels: interpretation of structure and the effects of processing. updated and translated by A Costa e Silva, Materials Park, OH: ASM International; 2018.

8. Y Zhongmin Research and development of high strength steel rebar in China.(2018) :14

9. AM Sage. Effect of vanadium, nitrogen, and aluminium on the mechanical properties of reinforcing bar steels. Metals Technology. 1976;3(1):65–70.

10. LL Teoh. Thermo-mechanical processing and microstructure of microalloyed steel bar and wire rod products. Journal of Materials Processing Technology. 1995;48(1):475–81.

11. AJ Deardo. Niobium in modern steels. International Materials Reviews. 2003;48(6):371–402.

12. TN Baker. Microalloyed steels. Ironmaking & Steelmaking. 2016;43(4):264–307.

13. S Vervynckt, K Verbeken, B Lopez, JJ Jonas. Modern HSLA steels and role of non-recrystallisation temperature. International Materials Reviews. 2012;57(4):187–207.

14. B López, B Pereda, F Bastos, M Rebellato, J Rodriguez-Ibabe. Challenges of Nb Application in Thermomechanical Processes of Steels for Long Products. In Trans Tech Publ; 2018. p. 386–93.

15. DP Escobar, CSB Castro, EC Borba, AP Oliveira, K Camey, E Taiss, et al. Correlation of the Solidification Path with As-Cast Microstructure and Precipitation of Ti,Nb(C,N) on a High-Temperature Processed Steel. Metallurgical and Materials Transactions A 2018;49(8) 3358–3372

16. SF Medina, A Quispe, P Valles, JL Baños. Recrystallization-Precipitation Interaction Study of Two Medium Carbon Niobium Microalloyed Steels. ISIJ International. 1999;39(9):913–22.

17. B Dutta, EJ Palmiere, CM Sellars. Modelling the kinetics of strain induced precipitation in Nb microalloyed steels. Acta Materialia. 2001;49(5):785–794.

18. H-J Kestenbach. Dispersion hardening by niobium carbonitride precipitation in ferrite. Materials Science and Technology. 1997;13(9):731–9.

19. E Courtois, T Epicier, C Scott. EELS study of niobium carbo-nitride nano-precipitates in ferrite. Micron. 2006;37(5):492–502.